New Rate Constants for Ten OH Alkane Reactions from 300 to 400 K: An Assessment of Accuracy

Neil M. Donahue* and James G. Anderson

Harvard University, Department of Chemistry and Chemical Biology, 12 Oxford St, Cambridge, Massachusetts 02138

Kenneth L. Demerjian

Department of Earth Atmospheric Sciences, State University of New York, Albany, New York

Received: December 16, 1997; In Final Form: February 10, 1998

OH alkane reactions play a central role in atmospheric and combustion chemistry, and accurate modeling requires accurate knowledge of their rate constants over a wide temperature range. We present data for 10 OH radical − alkane reactions over the temperature range 300−400 K and then combine our data with other literature data to find optimally estimated Arrhenius parameters using a modified Arrhenius form consistent with transition state theory. This modified form explicitly accounts for the loose modes in the transition state that cause curvature in Arrhenius plots. It thus fits data over a wide temperature range in a realistic manner, allowing precise comparison of data sets covering different temperature ranges. By comparing our data with other published data, we establish that most of these rate constants are now known to better than 5% accuracy over the 300−400 K temperature range.

Introduction

Reactions of alkanes and hydroxyl radicals (OH) play a central role in atmospheric chemistry; they are also canonical direct abstractions. Because they initiate hydrocarbon oxidation sequences and constitute the dominant OH sink in the atmosphere, the accuracy to which we know their rate constants limits the accuracy of atmospheric chemistry models. Furthermore, by measuring the temperature dependence of a series of OH alkane rate constants, we can test theories of radical molecule reactivity and refine schemes for predicting unknown rate constants.

We have measured rate constants for 10 OH−alkane reactions between 300 and 400 K (the alkanes are ethane, propane, *n*-butane, 2-methylpropane, *n*-pentane, *n*-hexane, cyclopentane, cyclohexane, cycloheptane, and cyclooctane). Some of these reactions have been studied many times, some only once, others only at room temperature, and still others not at all. By comparing our results with results from other studies, we conclude that many OH alkane rate constants are extremely well-known (5% accuracy or better).

Experimental Section

We conducted all experiments using a high-pressure flow system (HPFS). This system has been extensively described in the literature,[1,7] so we shall offer only a brief description here. A 10 m long, 12.36 cm diameter flow tube ensured a well-developed (laminar or turbulent) velocity profile, which we measured with a pitot-static tube. Velocity measurement accuracy was approximately 5% (accuracies are 67% confidence estimates). A large fraction of the nitrogen carrier gas flow recirculated through the system, but roughly 10% was exchanged for fresh carrier on each pass. The system was heated by heating tape wrapped around 7 m of the flow tube immediately upstream of the reaction zone. The temperature within the reaction zone was stable to approximately 3 K, except for a boundary layer extending at most 2 cm into the flow.

OH radicals were prepared by titrating H atoms with an excess of NO_2 in a quartz sidearm ∼50 cm upstream of the radical detection zone. The radicals flowed directly into the core of the flow through a thin, L-shaped injector. The spreading radical plume was well separated from the tube wall (typical diffusion times to the wall were of order one second, and reactions were studied over approximately 100 ms), so wall reactions were essentially nonexistent. We monitored OH in the core of the flow at five axial locations using laser induced fluorescence (LIF).

Each excess reagent was mixed with an inert tracer (CF_2Cl_2), which we measured in situ during each experiment using absorption at the 184.95 nm Hg line. The overall accuracy of the reagent measurement, including mixing and spectroscopic uncertainty, was approximately 5%. For each rate constant determination, the reagent-tracer mixture was injected into the HPFS, where it rapidly reached a maximum concentration and then declined exponentially over several minutes as fresh carrier was added to the system; this passively scanned the reaction through roughly 2 orders of magnitude of radical decay.

The experiments described here were carried out in low Reynolds number turbulence (p ∼30 Torr, R ∼4000, v ∼12 m/sec). We used gaseous reagents (Aldrich, except ethane from Matheson) without further purification, while liquid reagents were run through several freeze−pump−thaw cycles before use. Each rate constant was measured at least twice at each temperature, always in conjunction with nearly simultaneous measurements of the OH−ethane rate constant.

Our data analysis procedure is described in ref 7. In particular, we note that rate constant measurements made at the Reynolds numbers of this study were later found to be

* Corresponding author.

S1089-5639(98)00532-5 CCC: $15.00
Published on Web 04/15/1998

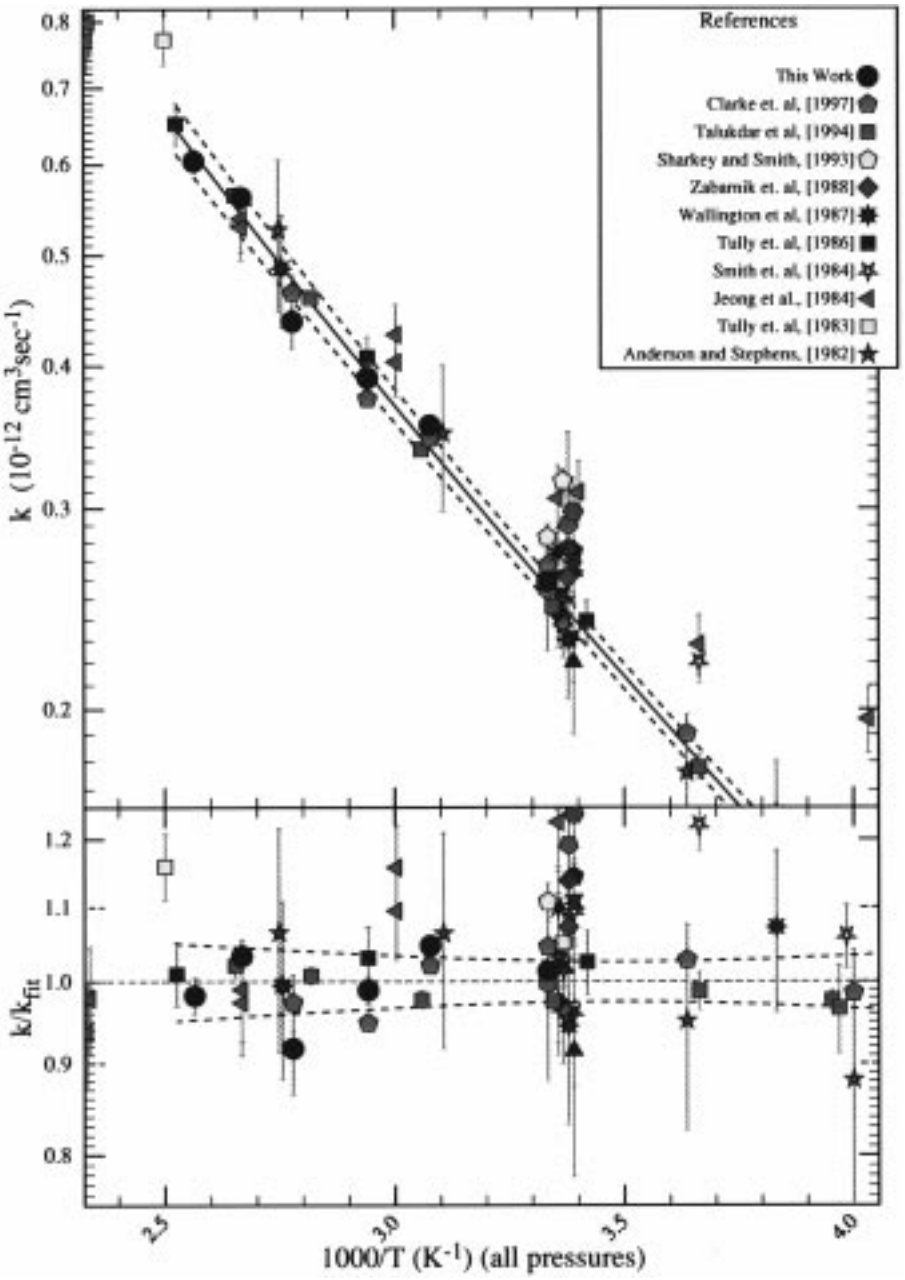

Figure 1. Data for OH + ethane vs (inverse) temperature. Our data are plotted as black circles. Other data from this lab are plotted as magenta symbols. Only temperature dependent studies are identified in the legend. The lower plot shows the ratio of each data point to a modified Arrhenius fit of selected data. The fit is also plotted in the upper plot. References for the cited data may be found in ref 4.

systematically low by 10%. The flow conditions employed in this study were thought to be turbulent at the time, but were later found to be transitional in nature. For reasons we do not understand, rate constants measured under these "semi turbulent" conditions for pressure independent reactions are consistently 10% lower than rate constants measured at other Reynolds numbers, in either laminar or turbulent conditions (e.g., Figures 7 and 8, $p = 30$ Torr, ref 7). Therefore, the ethane data reported in this work are scaled by 1.1 to correct for this systematic offset, while data for other reactions are corrected by comparison to the nearly simultaneous measurement of the OH + ethane rate. Not only does this correction eliminate the systematic offset, it reduces the overall scatter in the data, despite the added imprecision due to the second rate measurement. As discussed in ref 7, it also effectively eliminates all systematic errors from the UV absorption and the fluid dynamics, including diffusion effects and velocimetry errors.

Arrhenius Fitting

We shall present our data in conjunction with previous measurements and analyze a combined data set to obtain Arrhenius parameters. However, to do this in an unbiased manner, we must treat the natural curvature found in Arrhenius plots. Here we present a new modified Arrhenius function that more accurately accounts for the causes of the curvature.

Arrhenius plots for simple atom abstractions are curved because the interaction at the transition state involves the transformation of modes from relatively unrestricted forms (translations and rotations) to more restricted forms (rotations and vibrations) whose partition functions have different functional dependencies on temperature. Adding an arbitrary T^n term to the Arrhenius equation causes unrealistic behavior at low temperatures and produces an effective barrier that is not obviously related to a transition state energy. Instead we use a

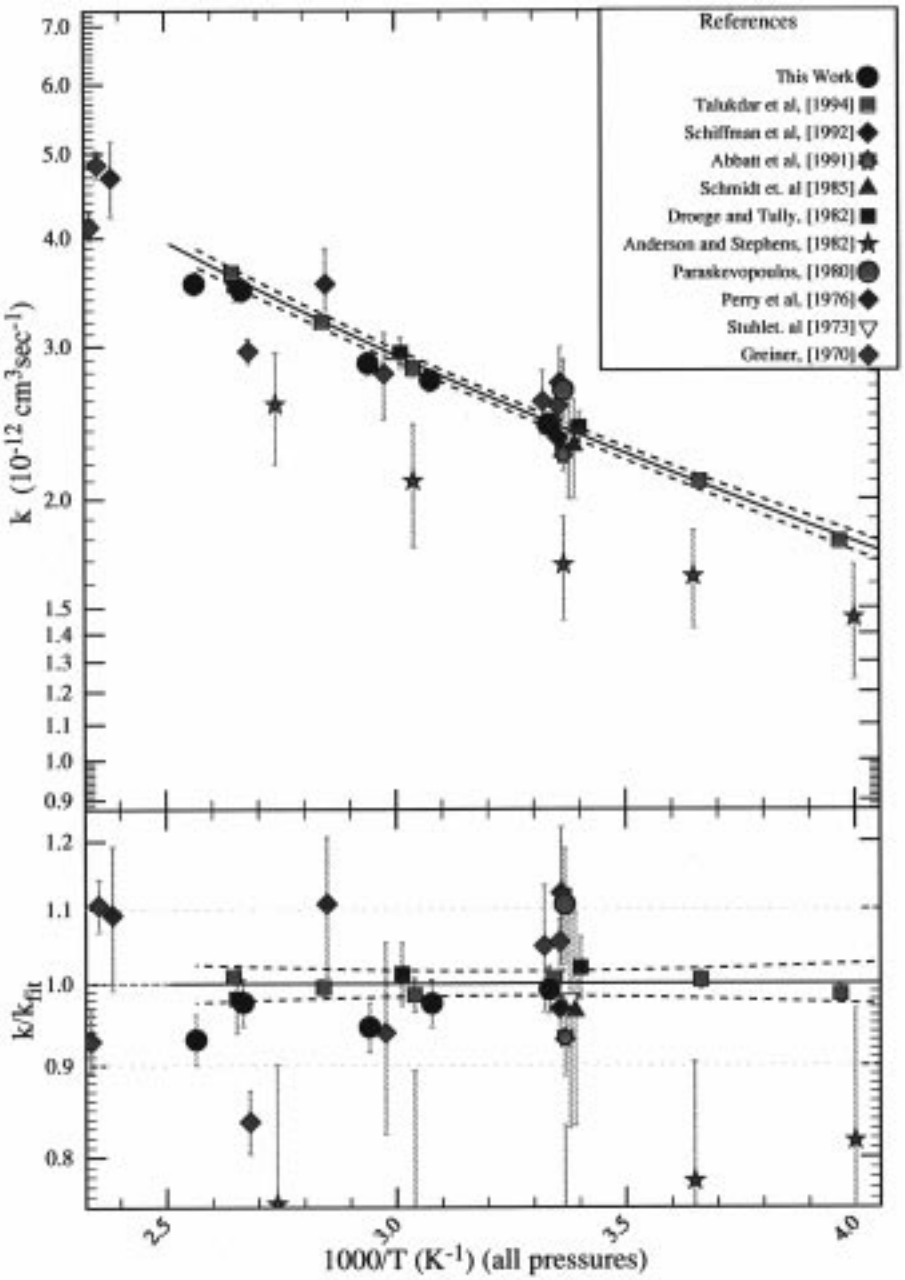

Figure 2. Data for OH + *n*-butane vs (inverse) temperature and a fit of selected data. Our data are plotted as black circles. References for the cited data may be found in ref 4.

functional form consistent with transition state theory, which explicitly treats these transformed modes. In particular, the transition state in OH−alkane reactions is almost linear in the C−H−O axis and bent along the H−O−H axes. Three modes are substantially transformed going from reactants to the transition state: one OH rotation becomes a modestly tight H−O−H bend, while two OH translations become loose (and essentially degenerate) C−H−O bends. The second OH rotation remains as an unhindered internal rotation. Of course, the collision frequency also changes with temperature.

Using transition state theory (ignoring tunneling) we calculate a functional form of

$$k(T) = \frac{Be^{-Ea/T}}{(T(1 - e^{-1.44\nu_1/T})^2(1 - e^{-1.44\nu_2/T}))} \qquad (1)$$

where ν_1 is the degenerate C−H−O bend frequency, in cm^{-1}, and ν_2 is the H−O−H bend frequency. Note that the barrier is expressed in terms of an activation temperature. This function behaves in a manner consistent with the data; in particular, it is roughly log−linear at low temperatures, then curves upward at higher temperatures as the loose bends activate. It allows us to introduce a minimum of bias when we compare a series of reactions studied over different temperature ranges. The activation energy is a true, zero-point corrected activation barrier, while the preexponential *B* factor is an inertial factor depending largely on the moments of inertia and reduced masses of the reactants and the transition state.

It would be folly to leave the frequencies in eq 1 as free parameters in a fit. We know of no data set that can actually constrain these frequencies; instead we use low-level ab initio calculations (UHF/6-31G**) to prescribe them. In this study, we use the same frequencies for all OH−alkane reactions (300 cm^{-1} for the C−H−O bends and 500 cm^{-1} for the H−O−H bend). While the UHF frequencies are similar for all of the reactions studied here, the actual frequencies are almost certainly

TABLE 1: Averaged Rate Constant Measurements (10^{-13} cm^3 s^{-1}) Adjusted to Reference Temperatures

alkane	300 K	325 K	340 K	360 K	375 K	390 K
ethane	2.59 ± 0.08	3.55 ± 0.11	3.90 ± 0.12	4.38 ± 0.23	5.61 ± 0.17	6.04 ± 0.18
propane	10.9 ± 0.3	13.7 ± 0.4	14.6 ± 0.4	16.0 ± 0.9	18.5 ± 0.6	18.3 ± 1.0
n-butane	24.3 ± 0.7	27.4 ± 0.8	28.7 ± 0.9		34.8 ± 1.0	35.4 ± 1.1
2-methylpropane	20.9 ± 0.6	23.8 ± 0.7	24.7 ± 0.9		26.2 ± 0.8	27.2 ± 1.4
n-pentane	39.8 ± 1.3	46.8 ± 3.3	45.9 ± 1.8	54.7 ± 1.6	58.3 ± 4.4	64.4 ± 3.7
n-hexane	54.5 ± 1.6	61.1 ± 1.8	62.3 ± 1.9	64.3 ± 4.5	73.3 ± 6.2	72.9 ± 2.2
cyclopentane	58.9 ± 2.6	63.5 ± 5.9	61.8 ± 1.9	76.4 ± 2.3	72.5 ± 3.8	75.3 ± 4.5
cyclohexane	76.6 ± 2.3	76.8 ± 2.3	78.4 ± 2.4	99.6 ± 3.4	90.6 ± 2.7	103 ± 6
cycloheptane	120 ± 3	134 ± 4	133 ± 4		149 ± 4	164 ± 14
cyclooctane	134 ± 4	150 ± 4	149 ± 4		166 ± 5	191 ± 6

correlated with barrier heights;[6] however, the configuration interaction treatment necessary to describe this phenomenon is beyond the scope of the current work. We therefore restrict ourselves to identical frequencies as the least biased approach. Also, while isotopic data are available in some few cases to extract temperature dependent branching ratios, this cannot be done for a sufficiently large set of reactions. We therefore apply eq 1 to all of the OH alkane reactions, even though several certainly have more than one active reaction channel.

Experimental Results

The entire data set comprises over 100 individual measurements of 10 separate reactions. It is available from the authors, in tabular and graphical form. To reduce the data to a manageable size, we have averaged them for presentation. However, simple binning and averaging would introduce a bias. Therefore, before averaging, we adjust each measurement to a reference temperature using our best estimate of the temperature dependence for the reaction. The temperature dependence is a result of fitting using the modified Arrhenius form described by eq 1. Furthermore, we include other published data to provide additional constraints for our fits. The purpose of fitting is to develop a best estimate of the true rate constant; comparison of fit parameters from different data sets is hazardous, as the parameters often have strong covariance and will generally be biased from one data set to the next unless treated as a whole. Instead, for each reaction we shall compare the mean residuals of each data set to our best estimate fit to the ensemble.

Our calibration reaction is OH + ethane. Figure 1 shows our data, spanning the range 300−400 K, along with an extensive set of literature values between 175 and 425 K. This reaction is very well understood. Fitting data from refs 5, 9−11, we find a barrier of (1042 ± 12) K and an inertial B factor of 1.24 ± 0.05 cm^3 K s^{-1}. The lower panel of Figure 1 shows the fractional residuals (data/fit) of all data to this fit. To assess the residuals numerically, we compute the mean fractional residual of each data set to the fit. The largest residual is from ref 9, at under 3%. Our data (which we have not used in this fit) fall 2% below the fit. In addition, room temperature measurements from refs 1, 7, and 8, all lie within 4% of the fit. Data from all these labs are particularly useful because they cover many of the reactions under discussion in this paper.

As a second example, we show our results for OH + *n*-butane in Figure 2. While the total data set is much more limited than for OH + ethane, data from most of the laboratories discussed for the OH + ethane reaction again constitute an excellent data set. In this case, three temperature dependent data sets all have average risiduals within 3% of the fit. The data from ref 2 are consistently 25% below the other data, while showing a similar activation energy. The same situation holds for propane, where data from ref 2 lie 13% below most data, again with little scatter, while for ethane that study agrees well with the literature and with our own data.

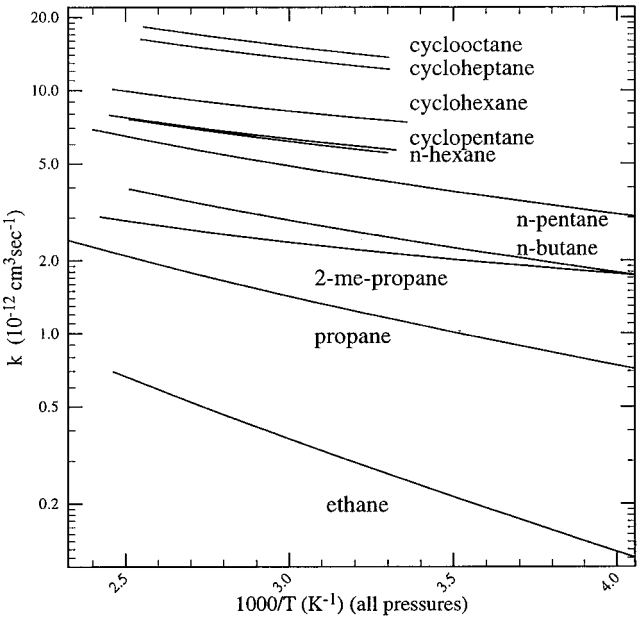

Figure 3. Modified Arrhenius plots for all reactions in this study. Each curve covers only the range of data used in the fit.

TABLE 2: Modified Arrhenius Fit Results

alkane	B (10^{-9} K cm^3 s^{-1})	Ea (K)
ethane	1.24 ± 0.05	1042 ± 11
propane	1.32 ± 0.03	616 ± 5
n-butane	1.68 ± 0.03	456 ± 4
2-methylpropane	0.75 ± 0.03	257 ± 11
n-pentane	2.46 ± 0.15	414 ± 18
n-hexane	2.10 ± 0.34	284 ± 53
cyclopentane	1.97 ± 0.41	253 ± 69
cyclohexane	2.36 ± 0.31	227 ± 43
cycloheptane	4.25 ± 0.59	256 ± 44
cyclooctane	4.98 ± 1.00	270 ± 62

[a] Two bends at 300 cm^{-1} and one bend at 500 cm^{-1} are treated explicitly (see text).

Reduced data for all of the reactions we studied are shown in Table 1, with 67% confidence estimates at each temperature. We use calculated temperature dependencies to interpolate our data to six temperatures between 300 and 390 K, chosen so data lie as close as possible to an interpolation point. The accuracy of these results depends on two factors: the accuracy of the ethane fit and the accuracy of the reagent preparation procedure. We estimate that each of these terms contributes roughly 5% to the overall accuracy beyond the quoted precisions.

The fit results are plotted in Figure 3 and shown in Table 2. While the clear progression of increasing rates with increasing carbon number is obvious, it is also evident that the rates arrive

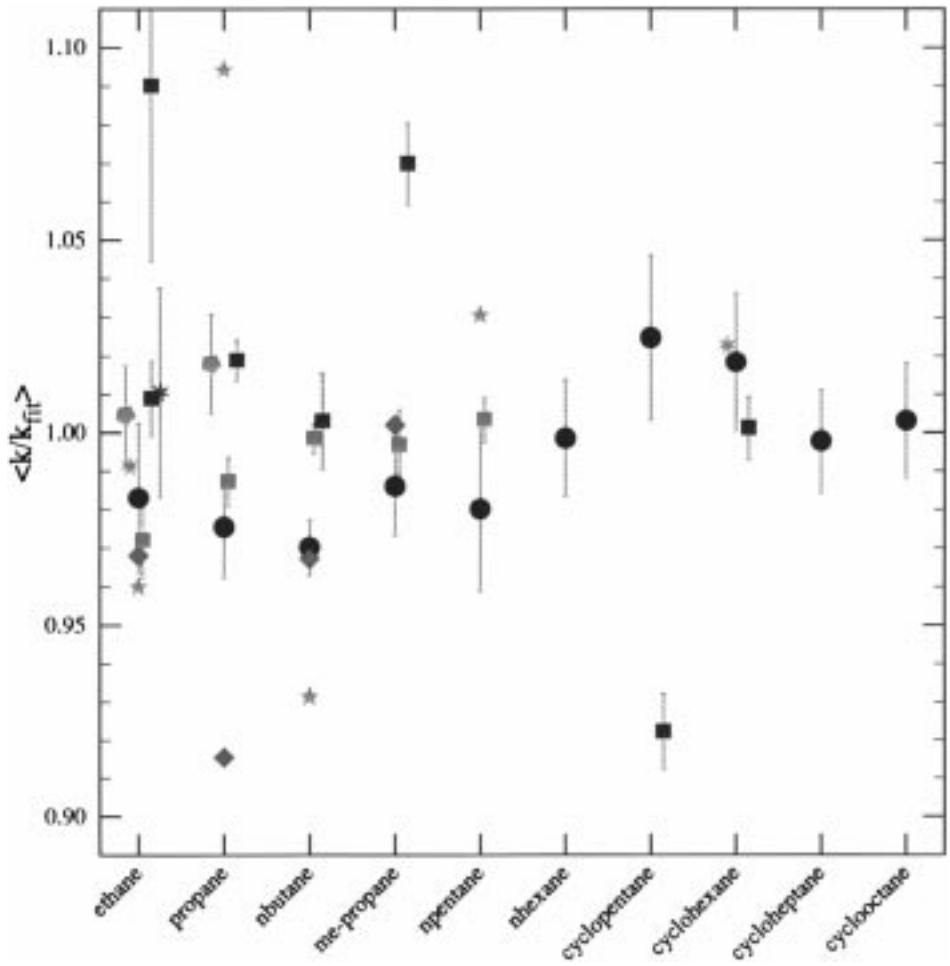

Figure 4. The average ratios of selected data sets to our fit functions for all reactions in this study. Our data are plotted as black circles. The entire range of the figure is ±10%. Data from different laboratories are plotted with different colors (This lab = magenta (symbols), Ravishankara = red (squares), Tully = blue (squares), Schiffman = cyan (diamonds), Wallington = green (star)).

at a common barrier quickly, leaving the increase almost entirely in the preexponential factor. For most of the reactions, the abstractions occur primarily from methylene groups, and the preexponential factors are loosely related to the number of methylene groups. Only one reaction, 2-methyl-propane + OH, stands out in this progression; both the barrier and the preexponential factor are unusually low. For this reaction, abstraction from the single methyne group dominates, leading to a low barrier and a low preexponential factor.

The reported uncertainties for the fit parameters must be treated with caution, as the parameters, including those held constant, are strongly covariant; however, we conclude that the temperature dependence for all of these reactions is well constrained over the ranges shown in Figure 3. Where low-temperature data are available, we can constrain the barriers to better than 20 K, while where the range is more limited we can constrain barriers to 50 K.

Literature Comparison

In Figure 4 we show the average ratio of selected data sets to our best fit for each reaction. The data sets selected for this figure are the same data used to perform the Arrhenius fits. Each laboratory shares a common color, and error bars show the error in the mean for each data set. The overall agreement with the fits is excellent: for the first three (C2−C4) reactions, all of the temperature dependent studies agree to better than 5%; for heavier alkanes, there are fewer constraints. The influence of our data varies from reaction to reaction. For ethane, propane, and *n*-butane we confirm already well-established rate constants. For 2-methyl-propane we resolve a 7% discrepancy between refs 10 and 9 in favor of the latter study. For *n*-pentane, cyclopentane, and cyclohexane we add a second temperature dependence to the literature; in the case of cyclopentane, a roughly 10% discrepancy remains to be resolved. For *n*-hexane, cycloheptane, and cyclooctane, our data are the first absolute temperature-dependent measurements.

Discussion

Given the large number of radical molecule reactions important to atmospheric and combustion chemistry, an accurate means of estimating rate constants has always been necessary. The OH−alkane abstraction reactions serve as the foundation for all schemes, both because they are in general the best known and the least complicated group of reactions. Estimation methods that account for variation in both radical and molecule reactivity can draw on data for alkane reactions with radicals such as oxygen, halogen, and hydrogen atoms for additional constraint. Most estimation methods can be grouped into one of three classes: those that rely on reaction enthalpy for prediction, those that rely on group properties for prediction (i.e. Atkinson et al. (ref 3)), and those that rely on ionic properties of the reagents.

In a companion paper (ref 6), we argue that the quantum mechanical interaction controlling both barrier heights and

preexponential factors is a curve crossing of two states. When the reactants are separated, these states can be identified as the ground state and an ionic state whose energy is approximately the difference between the ionization potential of the alkane and the electron affinity of the radical (IP-EA). Therefore, we contend that estimation methods based on molecular ionization potentials are the most closely related to the underlying quantum mechanics and thus the most likely to have predictive skill. Methods based on reaction enthalpy have some success because bond strengths and ionization potentials are strongly correlated in alkanes, while empirical methods based on group reactivity can also capture trends in ionization potentials.

A second issue is the method used to treat curvature in Arrhenius plots. It is common practice to add a T^n term to the temperature dependence of a rate constant to accommodate observed curvature. Most often the exponent is fixed at 2 (ref 3.) While the extra term does produce curvature, it has two severe shortcomings: it causes the fit parameter identified as the barrier height to differ markedly from the actual barrier, and it behaves unrealistically at low temperatures. We favor the method represented by eq 1, which is a highly simplified form of transition state theory. This function has the flexibility to fit observations while remaining firmly grounded in theory; the resulting barriers directly reflect real electronic barriers, and the functions extrapolate realistically to low and high temperatures.

Conclusions

We have presented temperature-dependent data for 10 OH−alkane reactions over the temperature range 300−400 K. Where data exist for comparison, the agreement is excellent. An evaluation of existing data for this series has led us to conclude that rate constants for most light alkane−OH reactions are very accurately known in this temperature range, with total errors as low as 5% in many cases. We have also offered a new functional form for fitting temperature dependent data that accommodates curvature in Arrhenius plots while remaining firmly grounded in transition state theory. These data, combined with our emerging theoretical understanding of radical−molecule reactivity, can serve as the foundatation for improved estimation methods for use in atmospheric and combustion chemistry.

Acknowledgment. We gratefully acknowledge the assistance of Edward Dunlea and Michael Bell in this work. This work was supported by grants from NSF, EPRI/ESERCO, and the DOE Distinguished Global Change Postdoctoral Program.

References and Notes

(1) Abbatt, J. P. D.; Demerjian, K. L.; Anderson, J. G. A new approach to free-radical kinetics: Radially and axially resolved high-pressure discaharge flow with results for OH + (C_2H_6, C_3H_8, *n*-C_4H_{10}, *n*-C_5H_{12}) → products at 297 K. *J. Phys. Chem.* **1990**, 94, 4566.

(2) Anderson, L. G.; Stevens, R. D. *Proceedings of 15th International Conference on Photochemistry*, Stanford, CA, June 27−July 1, 1982; Technical Report GMR-4087, EMV #130; General Motors Research Laboratories; Warren, MI.

(3) Atkinson, R. 1994. Gas-phase tropospheric chemistry of organic compounds. *J. Phys. Chem. Ref. Data*, *Monogr*. **1994**, *2*, 216pp.

(4) Atkinson, R. Gas-phase tropospheric chemistry of volatile organic compounds. 1. alkanes and alkenes. *J. Phys. Chem. Ref. Data* **1997**, 26, 215.

(5) Clarke, J. S.; Kroll, J. H.; Donahue, N. M.; Anderson, J. G. Reaction kinetics of OH with ethane, propane, and cyclopropane from 180K-360K: Defining frontier orbital interactions. *J. Phys. Chem.* **1998**. Submitted for publication.

(6) Donahue, N. M.; Clarke, J. S.; Anderson, J. G. Predicting radical-molecule barrier heights: the role of the ionic surface. *J. Phys. Chem.* **1998**. In press.

(7) Donahue, N. M.; Clarke, J. S.; Demerjian, K. L.; Anderson, J. G. Free radical kinetics at high pressure: A mathematical analysis of the flow reactor. *J. Phys. Chem.* **1996**, *100*, 5821.

(8) Schiffman, A.; Nelson, D. D., Jr.; Robinson, M. S.; Nesbitt, D. J. High-resolution infrared flash kinetic spectroscopy of OH radicals. *J. Phys. Chem.* **1991**, *95*, 2629.

(9) Talukdar, R. K.; Mellouki, A.; Gierczak, T.; Barone, S.; Chiang, S.-Y.; Ravishankara, A. R. Kinetics of the reactions of OH with alkanes. *Int. J. Chem. Kinet.* **1994**, *26*, 973.

(10) Tully, F. P.; Droege, A. T.; Koszykowski, M. L.; Melius, C. F. Hydrogen-atom abstraction from alkanes by OH. 2. Ethane. *J. Phys. Chem.* **1986**, *90*, 691.

(11) Wallington, T. J.; Neuman, D. M.; Kurylo, M. J. Kinetics of the gas-phase reaction of hydroxyl radicals with ethane, benzene, and a series of halogenated benzenes over the temperature range 234−438 K. *Int. J. Chem. Kinet.* **1987**, *19*, 725.